ELSEVIER

Contents lists available at SciVerse ScienceDirect

Journal of Wind Engineering and Industrial Aerodynamics

journal homepage: www.elsevier.com/locate/jweia



Experimental and numerical investigations of the flow around three different wall-mounted cylinder geometries of finite length



T. Uffinger a,*, I. Ali b, S. Becker a

^a Institute of Process Machinery and Systems Engineering, University of Erlangen-Nuremberg, Cauerstr. 4, 91058 Erlangen, Germany

ARTICLE INFO

Article history: Received 22 August 2012 Received in revised form 14 March 2013 Accepted 3 May 2013

Keywords: Wall-mounted square cylinder Laser Doppler anemometry SST SAS LES

ABSTRACT

Three-dimensional flow fields around three different wall-mounted cylinder geometries of finite length are evaluated. A combined approach which uses both experimental and numerical investigations is applied to provide an extensive database. For the experimental investigations, laser Doppler anemometry is used to determine the averaged velocity vectors and the RMS values of the velocities. For the numerical investigations, three different simulation techniques are applied. A shear stress transport (SST) turbulence model represents RANS approaches. A hybrid simulation technique combining Reynolds-averaged Navier–Stokes (RANS) and large eddy simulation (LES) features is realized by the scale adaptive simulation (SAS) model. The third type of numerical simulation is LES, which is able to capture the unsteady flow field in the entire computation domain. Experimental and numerical results are presented and compared with each other.

© 2013 Elsevier Ltd. All rights reserved.

1. Introduction

The interest in studies of the flow field around wall-mounted cylindrical structures of finite length is twofold. On the one hand, the investigation of the flow field around cylinders helps in understanding the fundamental physical phenomena of bluff body aerodynamics. On the other hand, cylinders or cylinder-like geometries can be found in many technical applications, such as antennas and attaching parts of vehicles, high-rise buildings and supports in internal and external flows. The basic configuration of this kind of application with a wall-mounted cylinder of finite length *L* and side length *D* in a cross-flow is depicted in Fig. 1.

The flow field around quasi-infinite and infinite cylinders has been a topic of intensive research. Examples of the numerous studies in this field are these of Williamson (1996), Zdravkovich (1997) and Matsumoto (1999). Nevertheless, findings concerning infinite cylinders are not necessarily transferable to finite geometries. For example, Wang and Zhou (2009) and Wang et al. (2009) found that the trajectories of the vortices in the wake of a finite cylinder differ from those of an infinite cylinder, which leads to a broadening of the wake. Not only are modifications of the flow field observed on comparing the flow around infinite and finite

cylinders, but also a change of the whole flow structure in the wake.

Although the three-dimensional flow structure around a finite wall-mounted cylinder is complex and different proposals for visualization have been put forward, the model following Wang (2004) is depicted in Fig. 2 as a basis for discussion, because it seems to display the relevant flow features.

Thus, four main flow features have to be distinguished: the horseshoe vortices stretching around the front base of the cylinder, base vortices at the wall in the near-wake of the cylinder, Kármán vortex shedding at half-height of the cylinder and the flow over the top of the geometry with its effect on the upper wake. According to Sau et al. (2012) and Bourgeois et al. (2011), the influence of the horseshoe vortices on the wake of the cylinder is weak and therefore is not considered in this paper. Additional information from the literature on the three remaining flow features is given in the following.

In contrast to infinite cylinders, a high-momentum fluid of the free stream enters the wake not only by laterally formed vortices but also by the flow passing the free end of the configuration. This leads to a downwash flow in the spanwise symmetry plane of the wake near the free end. Etzold and Fiedler (1976), Kawamura et al. (1984) and Sumner et al. (2004) proposed the existence of streamwise tip vortices as shown in Fig. 2, which are linked with the downwash. Sakamoto and Arie (1983) and Wang and Zhou (2009) assumed that the vertical vortices formed on the two sides of the cylinder and the flow over the top forms an arch-type structure as depicted in Fig. 3. There seems to be a consensus that

^b Institute of Fluid Mechanics, University of Erlangen-Nuremberg, Cauerstr. 4, 91058 Erlangen, Germany

^{*} Corresponding author. Tel.: +49 9131 8529464; fax: +49 9131 8529449. *E-mail addresses*: uf@ipat.uni-erlangen.de (T. Uffinger), irfan.ali@gmx.de (I. Ali), sb@ipat.uni-erlangen.de (S. Becker).

Nomenclature Greek symbols		L _{VK} Kármán length scale
		p unsteady pressure p _{stat, rel} static relative pressure
δ δ_1 δ_2 Δt ϵ λ_2 ν ρ ω Ω	boundary layer thickness boundary layer displacement thickness boundary layer momentum thickness time step size dissipation eigenvalue kinematic viscosity density turbulent frequency antisymmetric part of the velocity gradient	Re Reynolds number S symmetric part of the velocity gradient Sr Strouhal number T temperature Tu intensity of turbulence u, v, w, u_i unsteady velocities U, V, W, U_i time-averaged velocities U_{∞} free stream velocity U_{displ} displacement velocity $U_{\text{rms}}, V_{\text{rms}}, W_{\text{rms}}$ RMS values of the velocities x, y, z, x_i cartesian coordinates
Latin :	symbols	Abbreviations
A_i B C_w D F_j H H_{12} k L L_1 , L_2	area vector in <i>i</i> -direction width of integration surface drag coefficient cylinder side length force in <i>j</i> -direction height of integration surface boundary layer form factor turbulent kinetic energy cylinder height length of integration surface turbulent length scale	CFL Courant-Friedrichs-Lewy DEHS diethylhexyl sebacate DNS direct numerical simulation LES large eddy simulation LDA laser Doppler anemometry RANS Reynolds-averaged Navier–Stokes RMS root mean square SAS scale adaptive simulation SST shear stress transport

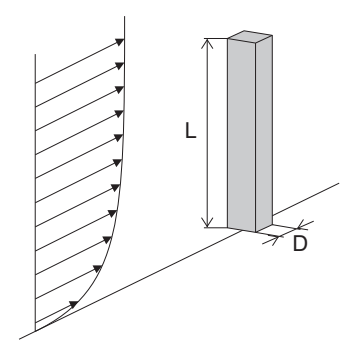


Fig. 1. Basic flow configuration: wall-mounted cylinder of finite length in a cross-flow.

with increasing length to side length or diameter ratio L/D the downwash increases (Sumner et al., 2004; Wang and Zhou, 2009). Nevertheless, only for small L/D ratios does the downwash in the spanwise symmetry plane reach the wall (Kawamura et al., 1984; Wang and Zhou, 2009; Bourgeois et al., 2011).

Etzold and Fiedler (1976) and Sumner et al. (2004) also found two counter-rotating vortices at the wall in the near-wake of the cylinder (Fig. 2). Their sign of vorticity is the opposite of that of the tip vortices, resulting in an upwash in the spanwise symmetry plane. The base vortices were confirmed by Krajnovic (2011). Wang and Zhou (2009) showed that the upwash induced by the base vortices is enhanced with increasing length to side length or diameter ratio L/D. Furthermore, the upwash is strongly dependent on the ratio of the boundary layer thickness to the cylinder length δ/L . While for very thin boundary layers no base vortices are evident (Fröhlich and Rodi, 2004; Bourgeois et al., 2011), they are strengthened with increasing thickness of the boundary layer (Wang et al., 2006).

In the region near the half-height of the cylinder, where the influence of tip and base vortices is weak, vertical vortices are formed at the side faces of the cylinder. The flow feature is

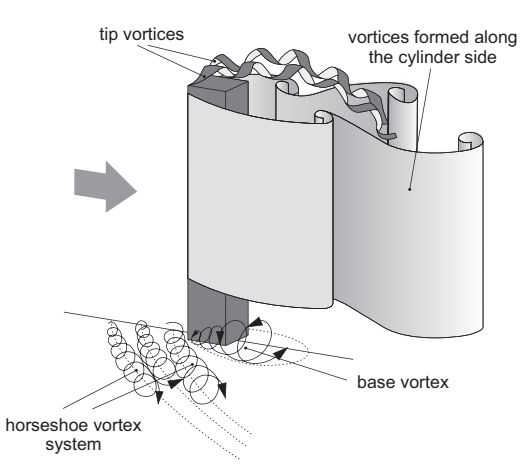


Fig. 2. Flow structures around a wall-mounted cylinder of finite length following Wang (2004).

comparable to the well-known Kármán vortex shedding of infinite cylinders (Wang et al., 2006; Wang and Zhou, 2009; Sattari et al., 2012; Krajnovic, 2011). The vertical vortices are schematically depicted in Figs. 2 and 3. Two different types of shedding are observed. In the first, a vortex is alternately formed and shed on one side of the cylinder (Kármán-type) (Fig. 3(a)). In the second, a vortex is formed and shed on each side of the geometry simultaneously (arch-type) (Fig. 3(b)). Both antisymmetric and symmetric vortices were observed along most of the axis of the cylinder by Wang et al. (2006), Wang and Zhou (2009) and Sattari et al. (2012), but antisymmetric shedding is much more probable in the halfheight region whereas symmetric shedding is preferentially found at the free end and near the wall (Wang and Zhou, 2009). Moreover, for small length to side length or diameter ratios L/D, symmetric vortices dominate the flow field downstream of the cylinder (Sakamoto and Arie, 1983; Okamoto and Sunabashiri, 1992).

Download English Version:

https://daneshyari.com/en/article/6757794

Download Persian Version:

https://daneshyari.com/article/6757794

<u>Daneshyari.com</u>